J. theor. Biol. (1993) **165**, 633–658

A Model for the Spatial Patterning of Teeth Primordia in the Alligator: Initiation of the Dental Determinant

J. SNEYD† ††, A. ATRI†, M. W. J. FERGUSON‡, M. A. LEWIS§, W. SEWARD‖ AND J. D. MURRAY¶

† *Department of Biomathematics, UCLA School of Medicine,* 10833 *Le Conte Ave., Los Angeles, CA* 90024-1766, *U.S.A.*, ‡ *Department of Cell and Structural Biology, University of Manchester, Manchester, U.K.*, § *Department of Mathematics, University of Utah, Salt Lake City, Utah* 84112, *U.S.A.*, ‖ *Department of Computer Science, University of Waterloo, Waterloo, Ontario, Canada and* ¶ *Department of Applied Mathematics FS*-20, *University of Washington, Seattle, WA* 98195, *U.S.A.*

(*Received on* 28 *January* 1993, *Accepted in revised form on* 21 *April* 1993)

We propose a mathematical model mechanism for the initiation and spatial positioning of tooth primordia in the alligator, *Alligator mississippiensis*. Our goal is to formulate and analyse a model that explains the spatial patterning of teeth primordia. In line with experimental evidence, jaw growth plays a crucial role in our model. This paper is concerned with the initiation of the first tooth in the lower jaw of the alligator, the dental determinant, one of the important elements in understanding dentition patterning. The model we propose is a caricature of the qualitative model proposed by Westergaard & Ferguson (1987), and describes the initiation of the dental determinant as a process controlled by jaw growth, the age structure of the epithelial cells in the developing jaw, and the age-dependent production of cellular adhesion molecules in the dental epithelium. The model incorporates both mechanochemical and reaction–diffusion mechanisms, and makes the important prediction that gradual changes in the mechanical properties of the epithelial cells are not sufficient to explain the spatial position of the dental determinant. The study of pattern formation in this growing domain demonstrates that simpler and more intuitive approaches to pattern formation can be misleading in the study of pattern formation in more complex situations such as the one studied here.

Introduction

One of the most important goals in the application of mathematics to biology is the understanding of how pattern and structure (both temporal and spatial) arise in biological systems. The mathematical investigation of developmental systems is an important aspect of this work; in most developmental situations, the process by which a complex, organized structure develops from a homogeneous group of cells is not well understood. The process of development is, *a priori*, one of self-organization, and although the immediate objective of research must be to discover the components of such self-organizing systems, the question of whether such components are sufficient in themselves to generate the required spatial structure is a question

†† Author to whom correspondence should be addressed.

0022–5193/93/024633+26 $08.00/0

that can optimally (and sometimes only) be answered by a mathematical investigation of the system. From this viewpoint, the mathematical study of developing systems is a study of sufficiency, and it is in this spirit that we approach the present work.

There are two principal approaches to the problem of how spatial structure arises in the developing embryo. The first, proposed by Turing (1952), involves the study of reacting and diffusing chemicals, or morphogens. It is now well known that such reaction–diffusion systems are capable of producing complex spatial patterns from an initially homogeneous state and this theory has been applied to a wide variety of biological systems (see Murray, 1989, for a detailed discussion and survey of pattern formation in reaction–diffusion systems). Often, although not necessarily, these theories have relied on the formation of a prepattern by some system of reacting and diffusion chemicals. Cells then determine their position by interpreting the local concentration of the chemical or chemicals (Wolpert, 1968, 1971, 1981), and differentiate accordingly.

More recently, a different class of model mechanisms for pattern formation in the developing embryo has been proposed, namely the mechanochemical models (Odell *et al.*, 1981; Oster *et al.*, 1983, 1985; Murray *et al.*, 1983; Murray & Oster, 1984*a*, *b*). These models are based on the mechanical properties of cells and the extracellular matrix and are capable of producing a rich array of spatial patterns (see Murray *et al.*, 1988 for a review, and Murray, 1989, for detailed discussion and references). However, although the components of the mechanochemical models are based firmly on measureable biological quantities, it is not realistic to suggest that these models can account for all aspects of morphogenesis. It is clear that mechanical, chemical, and diffusion effects are important in the pattern formation process and therefore a more complete understanding of the development of spatial pattern can only be gained by the construction of models that incorporate aspects of both the reaction–diffusion and the mechanochemical theory when dictated by known biological facts.

Here, we propose a model for the formation of the teeth primordia in *Alligator mississippiensis* that is based as much as possible on the known biological processes that underly tooth formation. Our model is in large part a mechanistic realization of a caricature of the descriptive model for tooth formation proposed by Westergaard & Ferguson (1987). Although our model is necessarily a caricature of the real biological system, which is still largely unknown and therefore much has to be assumed, it aims for greater biological plausibility at the expense of mathematical tractability. In constructing this model we wish to investigate whether certain mechanisms are sufficient to explain the observed pattern. This is not to claim the necessity of such mechanisms, but an understanding of what processes could possibly produce the pattern will lead to an enhanced understanding of the actual process.

Biological Basis of the Model

PREVIOUS MODELS OF TOOTH FORMATION

A number of descriptive models of tooth formation have been proposed; in general they fall into two categories—prepattern models (in which the pattern is imposed

from an external source) and what we shall call dynamic models, in which the pattern arises as part of the dynamics of the developing system.

In 1960, Edmund proposed the *Zahnreihe* theory of tooth formation (Edmund, 1960, 1962). He postulated that teeth in reptiles are replaced by initiation waves that proceed from the front to the back of the jaw. As each initiation wave passes a tooth position, it initiates a tooth. The row of teeth thus formed (all at different stages of development) is called a *Zahnreihe*. By controlling the timing between each new initiation wave one can obtain waves of replacement teeth that proceed either from the back to the front of the jaw or *vice versa*. As Osborn (1971) pointed out, this purely phenomenological model requires the previous determination of the tooth positions. Thus, there must be some prepattern mechanism that lays down a pattern of tooth initiation sites upon which the initiation wave may act. Interestingly, Edmund (1960) tentatively proposed the presence of a chemical transmitter, produced at the front of the jaw, that moves down the jaw in some sort of wave. Osborn (1970), however, showed that this is not actually necessary. Regular tooth replacement waves can be explained by a kinematic wave mechanism, in which the replacement waves are governed by the times between the initiation of each new tooth in a tooth family.

Although the *Zahnreihe* theory was accepted by most investigators at the time [see Osborn (1984) for references], Osborn (1971) demonstrated, first, that no known pattern of tooth initiation in embryos actually fits into the *Zahnreihe* theory, and second, that the data of Woerdeman (1919) (upon which Edmund's theory was based) was actually rearranged by Edmund to fit his theories. Osborn (1971, 1978, 1979) proposed a different model, the clone or clade model. In this model, any part of the dental lamina is capable of producing teeth, and tooth formation is initiated by growing clumps (or clades) of mesenchymal cells. The initiation of new teeth is directly related to the growth of the clade and each new tooth is surrounded by an inhibition zone that prevents nearby tooth formation; the final number of teeth is determined by the rate of growth of the clade as well as the size of the inhibition zone.

Recent work by Westergaard & Ferguson (1986, 1987, 1990) has demonstrated that, although many of the details of Osborn's model are incorrect, the fundamental approach of dynamic modelling of tooth formation is of great value. They have studied in detail the upper (Westergaard & Ferguson, 1990) and lower (Westergaard & Ferguson, 1986, 1987) dentition of *A. mississippiensis* from tooth initiation right through to the first erupted and functional dentition. Notwithstanding the early results of Röse (1894) and Woerdeman (1919) on *Crocodylus porosus*, this experimental work is the standard by which any model for tooth formation in alligators must now be judged. Their main conclusion (from the point of view of modelling tooth formation) is that tooth formation is directly related to growth. This result is in agreement with the work of Lumsden (1979) on mice, who showed that a complete molar dentition could be obtained from progenitor dental tissue grown in an artificial environment. Further, as in the Osborn model, there is a zone of inhibition around each developing tooth. Another important result of the work of Westergaard & Ferguson is that the initial sites of tooth initiation are not well defined before they

are separated by connective tissue. Thus the concept of a tooth family is not meaningful in the initial stages of dentition development. This is an immediate indication that the sites of tooth initiation are *not* laid down by a prepatterning mechanism, and that a dynamic model will be necessary to explain tooth initiation patterning.

Here, we propose a quantitative model mechanism for tooth formation. Experimental evidence requires that in this model mechanism, the pattern arises dynamically as a result of jaw growth and not as the result of a prepattern of tooth initiation sites. Thus the resultant model will have many conceptual similarities with the work of Osborn (1971, 1978, 1979). Our main task will be to relate molecular and cellular mechanisms at the level of the individual tooth to the macroscopic pattern. We thus hope to show that the postulated mechanisms are sufficient to explain the pattern of tooth initiation sites in *A. mississippiensis*.

DENTITION PATTERN

One of our aims is to reproduce the observed pattern of tooth formation in *A. mississippiensis* as detailed by Westergaard & Ferguson (1986). In particular, we propose to model the initiation sequence and positions of the first seven teeth in the right half lower jaw. An understanding of these is sufficient to understand the subsequent dentition sequence.

The first tooth (the dental determinant) in the right half lower jaw of *A. mississippiensis* forms in the anterior part of the jaw at the position of the third tooth family as shown in Fig. 1. It is *not* the most anterior tooth to form. Following teeth are initiated in a sequence towards the back of jaw but as the jaw grows in a regular manner, this initiation sequence changes to a regular alternation, with the new tooth closer to its older neighbour. Thus, the first seven teeth form in the pattern

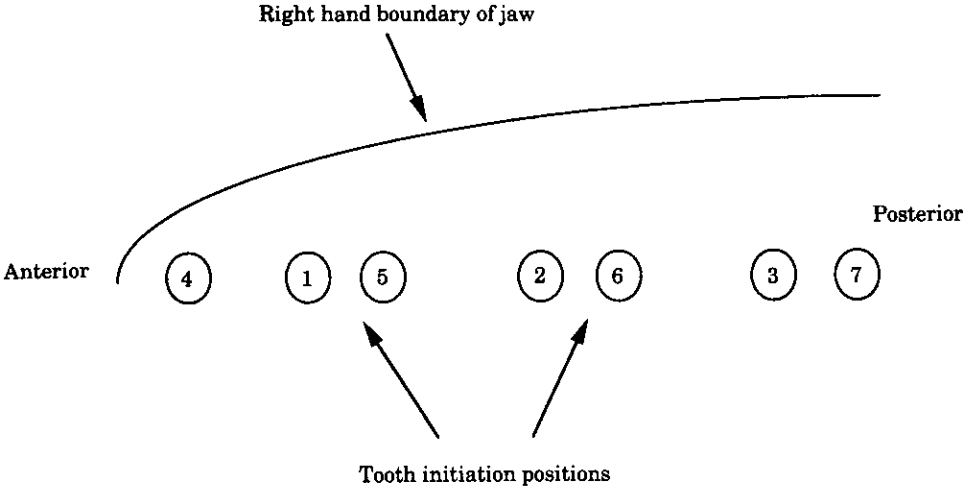

FIG. 1. The positions and initiation sequence of the first seven teeth in the right half lower jaw of *A. mississippiensis* (Westergaard & Ferguson, 1986).

shown in Fig. 1. There is very little variation from this pattern. Both the temporal and spatial sequences are extremely stable.

We limit ourselves to the first seven teeth for a number of reasons, the first being that to reproduce this pattern with a realistic model is already a major challenge. Further, the formation of subsequent teeth is complicated by the presence of resorbing older teeth, cell differentiation, and differential growth of the jaw. It is unrealistic to attempt to model the entire process at this stage.

MECHANISMS INVOLVED IN TOOTH FORMATION

The formation of each individual tooth is characterized by an extensive series of reciprocal epithelial–mesenchymal interactions (Kollar & Baird, 1969, 1970*a*, *b*; Kollar, 1981; Thesleff & Hurmerinta, 1981; Mina & Kollar, 1987; Lumsden, 1988; Thesleff *et al.*, 1988, 1989). These may conveniently be considered as proceeding in three overlapping stages (Kollar & Lumsden, 1979); initiation, morphogenesis and differentiation.

Tooth initiation: the evidence from recombination experiments

In the initiation phase, cell condensations appear in the epithelium and underlying mesenchyme (Thesleff & Hurmerinta, 1981; Westergaard & Ferguson, 1986). Although it was thought (Kollar & Baird, 1970*a*, *b*; Kollar, 1981) that tooth development was initiated by the mesenchyme, more recent results (Mina & Kollar, 1987; Lumsden, 1988) have shown that, in mice, it is the epithelium that initiates tooth development. Recombination experiments in mice (Mina & Kollar, 1987; Lumsden, 1988) have shown that early mandibular epithelium is capable of inducing tooth formation in non-odontogenic trunk neural crest cells as well as in (presumptively odontogenic) cranial neural crest cells. Conversely, early mandibular mesenchyme is not capable of inducing tooth formation in non-odontogenic epithelium. It thus appears that the mesenchyme becomes capable of forming teeth only after interaction with early mandibular epithelium. Although these results have not yet been demonstrated in reptiles, it is reasonable to assume that tooth development in reptiles is also initiated by the epithelium. Similar transplant experiments have been carried out with other skin organs, notably feathers and scales (for example, Dhouailly, 1975). The results demonstrate the crucial determinant role of the epithelium.

The results of Westergaard & Ferguson (1986) agree well with this sequence of events. Tooth formation is initiated by the dental determinant (tooth 1 in Fig. 1), some time before the rest of the teeth begin to form. A localized condensation of epithelial cells, the placode, forms over a uniformly dense dermis; this is consistent with the above results that suggest that tooth formation is initiated by the epidermis. The placode then induces a condensation of cells in the underlying mesenchyme, the papilla. In our model we shall be concerned only with the formation of the placode and papilla—the further development of each individual tooth, involving complicated spatial interactions, a further series of extensive epithelial–mesenchymal interactions, and cytodifferentiation, is not addressed.

Molecular and cellular mechanisms

The mechanisms underlying the three phases of tooth formation are not yet well understood. What is clear, however, is that the processes involved are extremely complex. In the presentation of their descriptive model, Westergaard & Ferguson (1987) give a brief overview of some of the molecular mechanisms that have a possible influence on tooth development. These include positional information, cell adhesion molecules, cytoskeletal changes, soluble factors, extracellular matrix, differential adhesion, and cell lineage. At this stage it is not possible to include all these possible processes. In our caricature model we shall incorporate only some of those mechanisms that contribute to the formation of the primordia, with the aim of determining which effects are sufficient for pattern formation.

Westergaard & Ferguson (1986) suggest that the initial thickening of the epithelium is perhaps a result of the expression of cell adhesion molecules or CAMs (Chuong & Edelman, 1985; Obrink, 1986; Takeichi, 1988). This suggestion is consistent with the results of Thesleff *et al.* (1988, 1989). They show that the changes in the expression of a cell surface proteoglycan are very similar to the developmental changes in the epithelium and the mesenchyme, namely, that the early odontogenically capable mandibular epithelium expresses the cell surface proteoglycan, but as the odontogenic potential passes to the mesenchyme, so does the expression of the cell surface proteoglycan. They conclude that, since these changes in expression are analogous to those of CAMs, it is possible that the cell surface proteoglycan acts as a CAM during part of the developmental process (Thesleff *et al.*, 1988). There is also recent evidence that increased cell division plays an important part in placode development (Kronmillar *et al.*, 1991) but it is not known exactly how such site-specific increased growth is initiated.

The expression pattern of a homeobox gene, Hox-8, in mice suggests that it plays a role in dental initiation (MacKenzie *et al.*, 1992). Hox-8 is expressed in the oral epithelium in the region of the dental placode. As it appears after the initial thickening of the epithelium, it is not the factor that initiates placode formation, but it is possible that it regulates the initial interaction between the epithelium and the mesenchyme that lead to the formation of the dental papilla.

Another homeobox gene, Hox 7·1, is expressed in the mesenchymal tissue of the developing jaw, in close association with sites of tooth initiation (MacKenzie *et al.*, 1991*a*, *b*). It appears that the thickening of the epithelium induces the expression of Hox 7·1 in the mesenchyme (possibly via Hox-8) and that Hox 7·1 is in turn at least partly responsible for the formation of the papilla. Hox 7·1 is not expressed in the dental epithelium. The expression of Hox 7·1 is broadly similar to that of tenascin (a matrix glycoprotein) and syndecan (a cell surface proteoglycan) (Thesleff *et al.*, 1989), and growth factors are also localized around the dental papilla (Partanen & Thesleff, 1989; see MacKenzie *et al.*, 1991*b* for discussion and references). Although none of these demonstrate exactly the same spatial or temporal pattern of Hox 7·1 expression, it is possible that Hox 7·1 regulates the formation of the papilla by regulating the expression of various extracellular molecules, growth factors and/or chemotactic factors.

SUMMARY OF THE BASIC BIOLOGY

The first tooth is initiated in the epithelium at a particular place in the anterior part of the jaw; the position of this dental determinant is the same in similar specimens. Epithelial cells are not very motile and the placode in the epithelium is the result of a thickening of the epithelial layer. The placode induces the formation of a papilla in the mesenchyme. Mesenchymal cells are motile and the papilla is a localized region of higher cell density. Although the mechanisms underlying papilla formation are complex, the aggregation is possibly partly a result of a chemotactic mechanism. The mesenchyme then becomes able to initiate tooth formation itself. The epithelium eventually loses the ability to initiate tooth development but the mesenchyme does not (during the developmental time scale we consider).

Subsequent teeth develop in the same way as the dental determinant (with the initial formation of a placode and the induction of a papilla in the mesenchyme with the associated expressions of Hox-8 and Hox 7·1). Since interstitial teeth always form closer to their older neighbour (cf. tooth positions 5 and 6 in Fig. 1), this suggests the presence of an inhibition zone around each developing tooth, a zone that decreases as the tooth grows older.

Further tooth formation is closely correlated to jaw growth (Westergaard & Ferguson, 1986, 1987, 1990). It seems that, at least in the early stages of tooth formation before the tooth family positions have been well defined (Westergaard & Ferguson, 1987, 1990), the tooth initiation positions depend on the relative amounts of jaw growth, with growth regulating the presence or absence of a tooth position. In other words, a new tooth will form if and only if there is enough room for it.

Model for the Initiation of the Dental Determinant

Because of the complexity of the processes involved in tooth initiation and the consequent model complexities we shall follow a piecewise approach to the model mechanism construction.

The initial part of the construction will focus on the initiation and spatial positioning of the dental determinant—the remainder of this paper will be concerned exclusively with this part of the process. The tissue interactions and the spatial positioning of the subsequent six teeth will be dealt with in subsequent publications.

THE MODEL ON A FIXED DOMAIN

Our ultimate goal is to relate the growth of the jaw to the initiation of the dental determinant. However, to study the model equations on a growing domain it is useful to first discuss the model for a fixed domain.

Preliminary assumptions

(i) The initiation of the dental determinant is governed solely by epithelial processes. Although it is known that odontogenic potential appears first in the epithelium, this of course does not necessarily mean that the development of

such potential is independent of tissue interaction processes. However, in the absence of evidence to the contrary, this is the simplest hypothesis to make.

(ii) The epithelium produces CAMs which tend to make epithelial cells stick together more closely. We shall model this as active traction exerted by epithelial cells on their neighbours (this is well documented in fibroblast cells: Harris, 1982; Harris *et al.*, 1980, 1981). The exact mechanism by which this traction is exerted is not germane for our model at this early stage. We model the result, not the cause. Although each cell produces more than one type of CAM it is sufficient to group them together and assume that only one type of CAM is produced and that the traction exerted by each cell is a function of the amount of CAM produced.

(iii) When epithelial cells are strained (with positive strain, i.e. stretching), they are stimulated to divide and when they do so, their production of CAM decreases. [Folkman & Moscona (1978) discuss the effect of cell shape on mitosis.] Thus, when a group of epithelial cells bunch together to form a placode, they strain the epithelial cells around them, and so they will be surrounded by a group of cells that are producing no CAM. This will act like an inhibitory zone around the placode.

(iv) As in the mechanochemical model of Murray & Oster (1984*b*; see also Murray, 1989), the epithelial sheet is assumed to behave like a visco-elastic fluid. Further, epithelial cells are connected to the basal lamina by elastic-like tethers.

Model mechanism equations

First, note that, because of jaw symmetry, it is only necessary to consider one side of the jaw. Second, the half-jaw, from the point of view of dentition, is essentially a one-dimensional structure. Thus we model the half-jaw presumptive dentition domain as a one-dimensional visco-elastic sheet of epithelial cells. Although the restriction to one dimension results in vastly simplified numerical calculations, we believe it captures qualitatively the features which would be exhibited by a curved jaw-like domain. We denote position along the jaw (measured from the base of the jaw) by x and time by t. Let

$n(x, t)$ = density of epithelial cells
$u(x, t)$ = displacement of epithelial cells
$c(x, t)$ = concentration of the CAM in the epithelium.

The mathematical model consists of equations governing the temporal and spatial variation of these variables which are assumed to be continuous (we consider a spatial scale such that the discrete nature of the cells may be ignored). We can relate all of the variables to specific biological entities.

The equations for the force balance and cell conservation in the epithelial and mesenchymal cell layers are based on those used by Murray & Oster (1984*a*, *b*; for a review see Murray, 1989). For clarity, we state each equation first in words and then give the mathematical formulation.

Cell conservation equation:

rate of change of epithelial cell density = convective flux

$$\frac{\partial n}{\partial t} = -\frac{\partial}{\partial x}\left(n\frac{\partial u}{\partial t}\right). \tag{1}$$

Force balance equation:

viscous forces + elastic forces + cell traction forces = external forces

$$\frac{\partial}{\partial x}\left[\mu\frac{\partial^2 u}{\partial x \partial t} + E\frac{\partial u}{\partial x} + \frac{n}{1+\lambda n^2}\tau(c)\right] = \sigma u n \tag{2}$$

where μ is the viscosity, E is the Young's modulus, and σ and λ are constants. A number of things should be noted:

(i) we have incorporated contact inhibition into the cell traction term. Because of the factor of $1+\lambda n^2$ in the denominator of the cell traction term, cell traction will decrease rapidly as the density of epithelial cells gets large.

(ii) the cell traction τ depends on the concentration of the CAM. We shall assume that traction is a linearly increasing function of the CAM concentration. The exact form of $\tau(c)$ used is given in the Appendix.

(iii) The term $\sigma u n$ on the right-hand side represents the connection of the epithelial cells to the basal lamina by elastic tethers. It serves as a restoring force, preventing excessive cell displacements.

CAM equation:

rate of change of CAM concentration = diffusion − degradation + strain-dependent production

$$\frac{\partial c}{\partial t} = \alpha\frac{\partial^2 c}{\partial x^2} - kc + F(u_x) \tag{3}$$

where $F(u_x)$ has the approximate shape shown in Fig. 2. The exact form used is given in the Appendix. Note that we are assuming that the production of CAM is independent of the cell density. The diffusion term in (3) should not be interpreted as direct intercellular diffusion of CAM; it is unlikely that CAM molecules move from cell to cell in the epithelial layer. However, production of CAM in one cell may increase the production of CAM in neighbouring cells, resulting in an effective intercellular movement. The diffusion term is merely a particularly simple way to model this movement.

These equations are discussed at greater length in the Appendix.

Behaviour of the model

A spatially homogeneous steady-state solution (i.e. one that is constant in space) of the model equations is given by $n = n_0$, $u = 0$, $c = c_0 = F(0)/k = F_0/k$ (cf. the Appendix). This corresponds to the unstressed state. Here, n_0 is the density of the epithelium in the unstressed state and is not determined from the model equations;

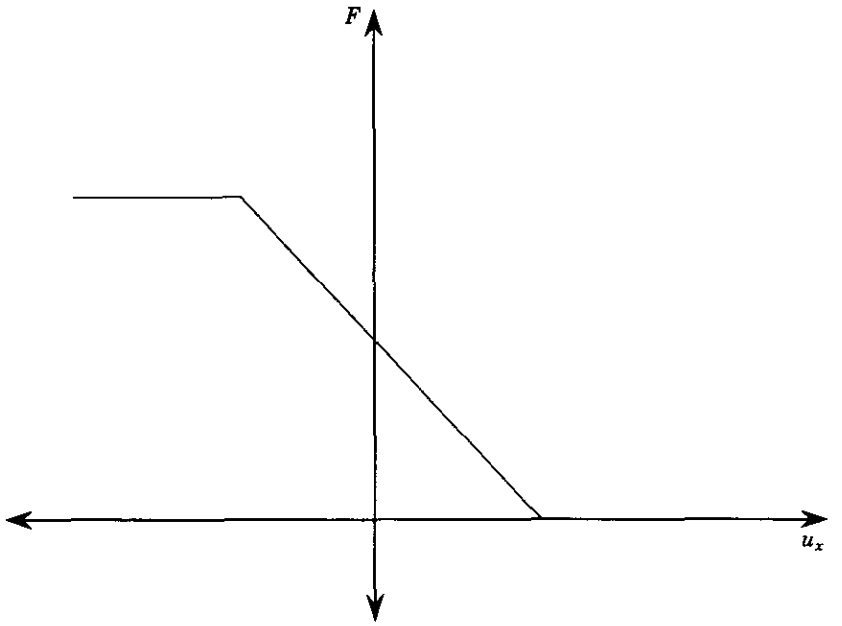

FIG. 2. The qualitative shape of the function $F(u_x)$. The exact form is given in the Appendix. According to this function, the rate of CAM production decreases when the cell is strained with positive strain, and increases when the strain is negative. For convenience, F is assumed to be piecewise linear.

n_0 must be measured experimentally; it is one of the model parameters. From the linear stability analysis (see Appendix) it can be seen that, for certain values of the parameters, the unstressed steady state is unstable. Thus, small random perturbations from the steady state may grow, resulting in a stable spatial pattern in the epithelial cell density. Some typical results are shown in Fig. 3. This mechanism for the production of the placode is similar to that proposed by Belintsev *et al.* (1987).

From the result in Fig. 3 we see that the model on a fixed domain can predict the formation of a local region of high epithelial cell density in the middle of the domain. This would be interpreted as the formation of a placode in the middle of the domain. This placode arises spontaneously as the result of instabilities in the model equations, and it forms in the middle of the domain. The spatial pattern is not a result of spatial heterogeneities in the model equations. However, on a *fixed* domain, the model predicts the apperance of the first tooth in the wrong place. The dental determinant does not appear in the middle of the jaw, but anterior to it. By solving the model on a growing domain, we shall show how a placode may form in a more anterior part of the jaw.

THE MODEL ON A GROWING DOMAIN

To simulate the effect of jaw growth on the dynamics of the pattern formation we must apply the mechanism on a growing domain. This requires some further assumptions.

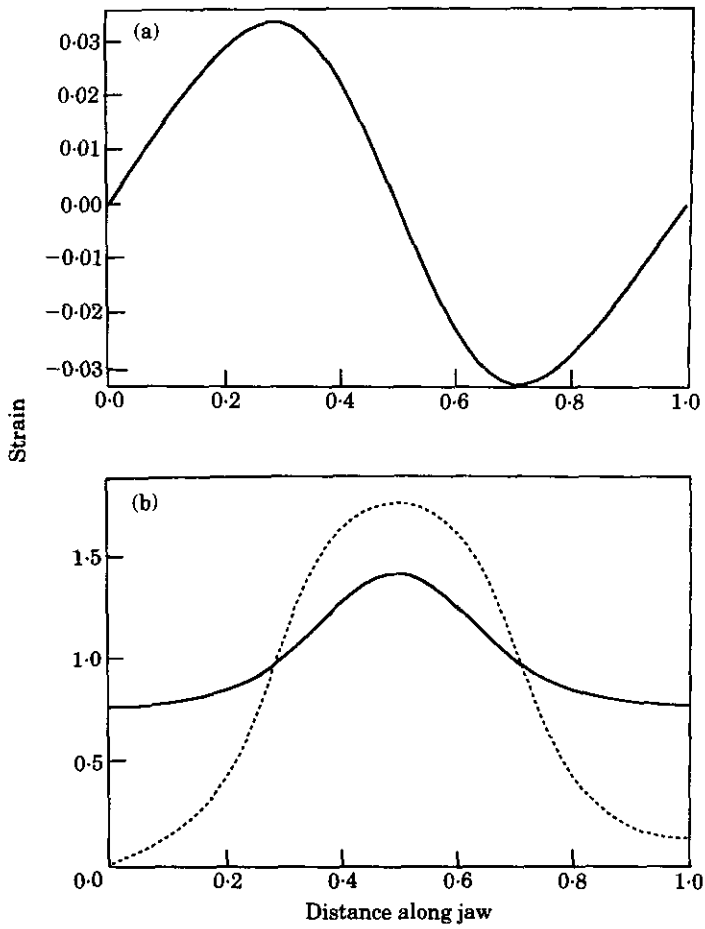

FIG. 3. Numerical solution of the model equations on a fixed domain of length 1, with dimensionless parameters $\tau_0 = 0{\cdot}7$, $\tau_1 = 0{\cdot}1$, $\lambda = 0{\cdot}1$, $\gamma_c = 0{\cdot}1$, $\kappa = 15{\cdot}0$, $\alpha = 0{\cdot}01$ and $\sigma = 6{\cdot}13$. (b) Shows the cell density (n) and the concentration of the CAM (c), while (a) shows the strain. As shown in the Appendix the parameters are chosen so that the mode $\cos(2\pi x)$ is linearly unstable. The initial conditions for n and c were $n = c = 1 - 0{\cdot}1\cos(2\pi x)$. The initial conditions for u and u_t were $u = 0$, $u_t = 0$. The linear instability results in the stable spatial pattern shown here. This stable pattern clearly reflects the underlying linear instability. The stable pattern develops by $t = 10$, corresponding to a real time of about 3 hr. (—), n (cell density); (— – —) c (concentration of CAM).

Further biological assumptions

(v) We assume that there is an age structure in the epithelial cells along the jaw, with younger cells at the back of the jaw, and older cells towards the tip, i.e. cells at the back of the jaw have, on average, divided more recently than cells at the tip. We shall model this age structure as a linear relationship between position along the jaw and cell age. This linear relationship is clearly a gross simplification. However, it appears that there is more jaw growth towards the

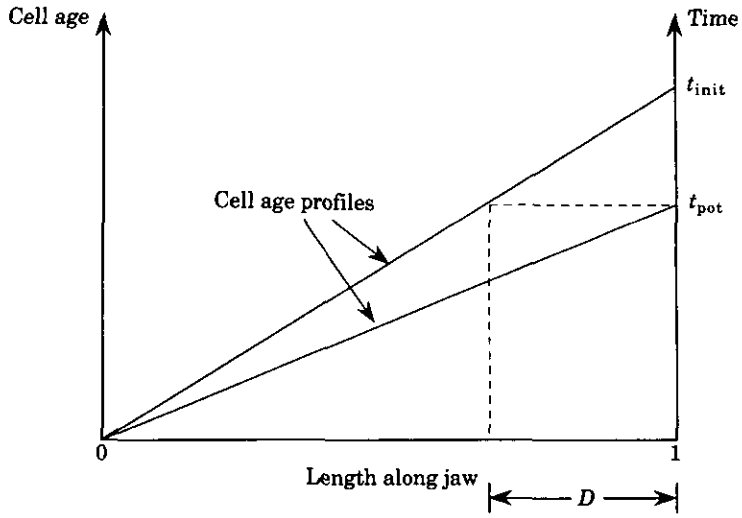

FIG. 4. Schematic diagram of the double-threshold potentiation–initiation hypothesis. The age of the cells along the jaw is assumed to be a linear function of position, as shown by the cell age profiles (the length along the jaw is measured from the jaw posterior; 0 corresponds to the base of the jaw, and 1 corresponds to the tip of the jaw). Because we control jaw growth by scaling the variables, always solving the model equations on the domain [0, 1] (cf. the Appendix), the slope of the cell age profiles increases with time. Cells older than t_{pot} are potentiated; they are capable of producing CAM at a higher rate, but do not yet do so. When the cells at the tip of the jaw reach age t_{init} they start producing CAM at a high rate, and stimulate all the potentiated cells to do likewise. This results in a region towards the anterior of the jaw (marked *D* here) in which all the cells are producing CAM at a higher rate. It is in this region that the dental determinant will form.

jaw posterior, and thus the assumption of a monotonic gradient in average cell age along the jaw is not unreasonable.

(vi) The rate at which a cell produces CAM is a function of its age. We shall assume that

(a) When each cell reaches a certain age, t_{pot}, it becomes *potentiated*, that is, it has the potential to produce CAM but does not necessarily do so.
(b) When each cell reaches the age $t_{init} > t_{pot}$, it begins CAM production.
(c) When CAM production begins in a particular cell, all the neighbours of that cell that are potentiated also begin CAM production.

Combining these assumptions gives the following scenario for CAM production, that we call the *potentiation–initiation double threshold* scenario: initially there will be little CAM production along the length of the jaw. At a later time, $t_{init} > t > t_{pot}$, there will be a region at the front of the jaw where the cells are potentiated but have not yet been activated. At time $t = t_{init}$, CAM production will be initiated at the front of the jaw and spread rapidly through the potentiated cells, resulting in a region of high CAM production towards the front of the jaw. A schematic diagram of this double-threshold scenario is given in Fig. 4.

Although it might appear that this assumption about the CAM production of the epithelial cells is unduly complicated, it turns out that it is the simplest hypothesis

that will result in the appearance of the dental determinant in the correct place. As there is no experimental evidence demonstrating such a complicated CAM production schedule, this assumption may thus be interpreted as a specific model prediction.

As we saw before, linear instabilities in the model on a fixed domain give rise to a local increase in cell density in the middle of the domain. Our goal is to show how the growing domain can skew the aggregation towards the jaw anterior. Once we have determined parameter values that give the correct instability for the model on a fixed domain, we hope to be able to use those same parameters on a growing domain and obtain the correct pattern as a result of the inherent asymmetry of the jaw.

Difficulties caused by the growing domain

It must be emphasized that the growing domain introduces severe modelling difficulties. The steady state is no longer uniform, since it is now a function of x and it is difficult, if not impossible, to calculate analytically. This in turn implies the linear stability of the steady state may not be calculated analytically. Hence, an investigation of the model behaviour is almost entirely dependent on numerical calculations. One of the more interesting results of this work is the demonstration that an intuitive understanding of pattern formation processes on fixed domains is not always useful for an understanding of how the model will behave in more complicated situations. Maini *et al.* (1992) demonstrate this clearly for a cell-chemotaxis model.

MODEL PARAMETERS

A serious problem with any morphogenetic model at this stage is that values for the parameters are not known, many not even approximately. Thus, when performing numerical simulations, we are forced to use parameter values that can not be directly justified by reference to experimental data. In these circumstances, although we find parameter values that work (that is, demonstrate appropriate linear instability) it is usually unclear whether or not these values are biologically reasonable. On the other hand, as can be seen from the Appendix, the behaviour of the model is dependent only on dimensionless groups of parameters. Thus, we may compensate for changes in one parameter by changes in another. As we shall see, specification of the values for the dimensionless parameter groupings does not uniquely determine the parameter values.

We can reasonably estimate five of the parameters in the model as follows.

L: Westergaard & Ferguson (1986) have shown that the dental determinant forms when the jaw is approximately 0·5 mm long. We thus choose $L = 0{\cdot}1$ mm, and look for the appearance of the first placode when the domain is $5L$ long. The appearance of the placode at the correct jaw length is not a model prediction—it is built into our numerical simulations.

n_0; This is based on the assumption that each epithelial cell has the same mass as a cube of water, with side 2 μm. In our one-dimensional strip of cells there are therefore 500 cells per millimetre, giving the above value for the density.

c_0; Although there is no quantitative data on the concentrations of CAM present in the developing jaw, it is reasonable to assume that these concentrations are relatively low. We assume that, in the unstressed state before activation, the resting level of CAM is 1 nM.

α; Again, there are no data on the effective intercellular diffusion coefficients of CAM in the epithelial layer, but it is reasonable to assume that this diffusion is low. We choose the diffusion coefficient to be spatially homogeneous with a value of 10^{-8} cm^2 sec^{-1} = 0·0036 mm^2 hr^{-1}.

τ_0; The traction forces exerted by fibroblast cells have been measured at approximately 10^{-5} N per mm of cell edge (Harris *et al.*, 1980). The traction forces exerted by epithelial cells are considerably less (Harris *et al.*, 1981) so we shall assume that each epithelial cell is capable of exerting a force of 10^{-7} N per mm of cell edge. Assuming that the cells have 2 μm sides, the total force exerted by each cell on its neighbour is 2×10^{-10} N = $2{\cdot}6 \times 10^3$ g mm hr^{-2}. Dividing by n_0 then gives the above value for τ_0.

In summary we have $L = 0{\cdot}1$ mm, $n_0 = 4 \times 10^{-9}$ g mm^{-1}, $c_0 = F_0/k = 1$ nM, $\alpha =$ 0·0036 mm^2 hr^{-1}, and $\tau_0 = 6{\cdot}5 \times 10^{11}$ mm^2 hr^{-2}.

Next, we present values for the dimensionless parameter groups that work. We shall then attempt to interpret these values in terms of biologically measurable processes. Unfortunately, at present such an attempt can only be partially successful; a more rigorous determination of parameter values for this system is a major problem that will have to be addressed in the future. Fortunately, even without this rigour, important qualitative results may be obtained.

Referring to the Appendix, we see that the desired linear instability occurs when $\tau_0 n_0/E = 0{\cdot}7$, $\tau_1 n_0 F_0/(kE) = 0{\cdot}1$, $\lambda n_0^2 = 0{\cdot}1$, $E/(k\mu) = 0{\cdot}1$, $F_1/F_0 = 15{\cdot}0$, $\alpha/(kL^2) = 0{\cdot}01$, $\sigma n_0 L^2/E = 6{\cdot}13$ where all the parameters here are dimensional. This linear instability is robust; the parameter groupings may be varied by, in some cases, as much as 100% in either direction without losing the desired linear instability. With these values we can solve for the other parameters. The most important is the ratio E/μ as this sets the time scale of the problem. It turns out that $E/\mu = 3{\cdot}6$ hr^{-1}. Thus, a dimensionless time of 3·6 corresponds to a dimensional time of 1 hr. The time scale of pattern formation in the model and in experiment can then be compared.

Another important ratio is $\tau_0/\tau_1 = 7$ nM which determines how sensitive the traction is to the concentration of CAM.

The value for E turns out to be $3{\cdot}7 \times 10^3$ g mm hr^{-2}, and so $\mu \approx 1 \times 10^3$ g mm hr^{-1}. In principle, the values for E and μ can be tested for consistency with experimentally determined values for the mechanical parameters. Such a consistency test will have to wait until more experimental data on these parameters becomes available. The same is true for the parameters σ and k, while λ has no direct biological interpretation—it relates to cell–cell inhibition in the cell traction.

NUMERICAL RESULTS

As described in the Appendix we set up a line of epithelial cells in one spatial dimension and solve the model by a stepwise approach, in which the length of the

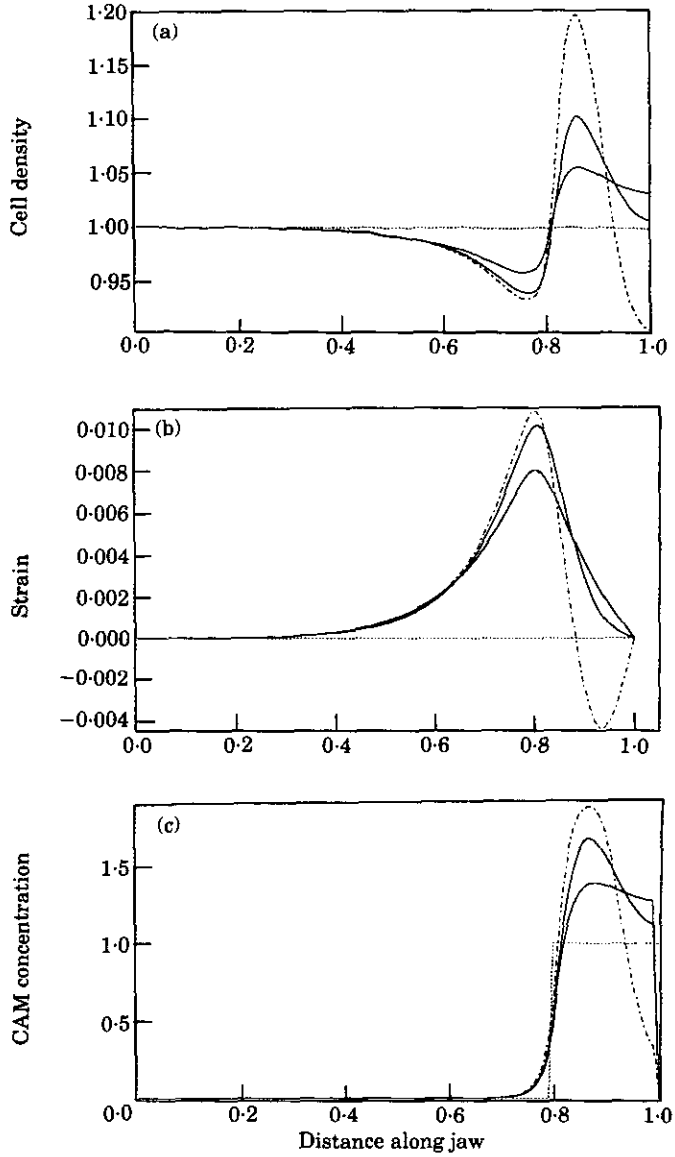

FIG. 5. Numerical solutions of the model equations on a growing domain. (a) Shows the epithelial cell density, n, (b) shows the strain, u_x, and (c) shows the CAM concentration, c. Details of the numerical simulation are given in the text and the Appendix. The relative times corresponding to these curves at $t = 0$ min, $t = 34$ min, $t = 80$ min, and $t = 280$ hr (the steady state), where $t = 0$ min corresponds to the activation of the epithelial cells at the anterior of the jaw. Thus, at $t = 0$, a region of cells at the jaw anterior (cf. Fig. 4) have been activated and are producing CAM, while those toward the back of the jaw are not. Note the presence of a placode in the anterior of the jaw which is surrounded by a region of low cell density. The CAM is concentrated in the region of the developing placode.

domain grows in a number of discrete steps. Recall that the age structure of the cells along the jaw is assumed to follow a linear relationship, as shown by the straight lines in Fig. 4, with cell age increasing towards the anterior of the jaw. Recall also that the model equations are always solved on the domain [0, 1], with domain growth being controlled by the scaling of the dimensionless parameters $\alpha(\propto L^2)$ and $\sigma(\propto L^{-2})$. If the slope of the cell age profile is given by s, it then follows that s will be a function of time. Furthermore, the rate of change of this slope, ds/dt, will be inversely (but not linearly) related to the rate of jaw growth.

Given these constraints, we choose the potentiation time, t_{pot}, and the initiation time, t_{init}, such that when the jaw is 0·5 mm long, the cells at the tip of the jaw are activated, and CAM production spreads rapidly along the front fifth of the jaw. Results from this simulation are shown in Fig. 5. From this figure it can be seen that CAM production begins in the front of the jaw at time $t = t_{init}$ and a local increase in epithelial cell density forms spontaneously in the anterior part of the jaw. We interpret this increase as the placode of the dental determinant. It can also be seen that, although CAM levels are initially high throughout the entire jaw anterior, they quickly concentrate in the region of the developing placode, reinforcing placode formation. This concentration of CAM is the result of strain modulation of CAM production. A stable state is reached in which non-linear effects balance the linear instabilities that are the immediate cause of the spatial heterogeneity. The placode is surrounded by a region of low cell density, which acts as an inhibition zone.

THE DOUBLE THRESHOLD MECHANISM

As we pointed out before, the potentiation–initiation double threshold mechanism is a complex hypothesis about the age dependency of CAM production. In fact, by making this hypothesis we are essentially converting the problem on a growing domain to a problem on a fixed domain, albeit with more complicated boundary conditions.

However, one crucial result of the numerical simulations is that simpler hypotheses, in which the concentration of CAM in the anterior of the jaw increases gradually, simply do not work. For the sake of argument let us consider one such simpler hypothesis, namely that the rate of CAM production is directly proportional to the age of the cell. CAM production would then be a linear function of distance along the jaw. An intuitive argument, based on the linear stability analysis of the model on a fixed domain, might run as follows:

(i) the homogeneous steady state of the model on a fixed domain, with $c = c_0$, is stable when the length of the domain is less than a certain threshold length, L_t say:

(ii) at early times, CAM production will be low in the posterior of the jaw. The concentration of CAM will be close to c_0 only in a small part (length less than L_t) of the anterior of the jaw:

(iii) thus, at early times, the steady state should be linearly stable:

(iv) at some later time, the part of the domain where $c \approx c_0$ will become greater than L_p, and linear instabilities will appear in that part of the domain. This will lead to the formation of a local increase in cell density in a region towards the anterior of the jaw.

Although this argument seems intuitively reasonable, numerical computations to date do not agree. In fact, a significant localized increase in cell density appears at the tip of the jaw, well before any linear instabilities develop, resulting in the appearance of a placode in the wrong place at the wrong time. Extensive numerical simulations confirm that any model in which the mechanochemical properties of the cells along the jaw vary gradually as the jaw grows will result in similar behaviour. A placode will appear in the correct place *only* if the mechanochemical properties of all the cells in the anterior of the jaw are changed suddenly. Thus, unless CAM production in the jaw anterior increases on a time scale much faster than that of jaw growth, an incorrect pattern will form.

Although this is a rather negative result, it focuses our attention again on the fact that simpler models on fixed domains can not necessarily be extrapolated to explain pattern formation on growing domains. This important aspect will have to be considered carefully when complicated developmental processes are studied with models on fixed domains.

MODEL PREDICTIONS

The most important prediction from our model arises from the above discussion. If the placode formation is the result of mechanical forces generated by the epithelial cell layer, and if these mechanical forces are mediated by a cellular adhesion molecule, then the model predicts that the CAM will suddenly appear in the region of the dental determinant immediately prior to the development of the placode. This is, in principle, a testable hypothesis, and is an obvious way in which the present model may be refuted (or encouraged).

The model also predicts that both the placode and the distribution of CAM concentration will initially be considerably more spread out than in the final placode. Testing of this prediction will require the measurement of cell densities and CAM concentrations on a very small time scale, that of hours (or perhaps even minutes), and may thus be extremely difficult. However, for a full understanding of this developmental process such experiments will eventually have to be carried out.

According to the model, initiation of the dental determinant will be considerably disrupted by removal of certain portions of the dental epithelium. If a portion of epithelium is removed from the tip of the jaw just prior to the formation of the dental determinant, the model predicts that the formation of the placode will be delayed by a time dependent on the amount of tissue removed and its position will be changed. If a large amount is removed, the model predicts that the dental determinant will still form, but at a later time and displaced towards the jaw posterior. The removal of a small strip of epithelium prior to the formation of the dental determinant will also have a considerable effect, even if that strip does not include the part of the jaw

where the placode will eventually form. If the strip is removed anterior to the place where the placode will form, placode formation will again be delayed and shifted to the posterior of the jaw. If the strip is removed posterior to the place where the placode will form, the effect of placode formation may be negligible.

Further tests of the model will involve a detailed investigation of the age structure of the cells along the developing jaw, the relationship between cell age and CAM production, and the importance of tissue interaction processes in the formation of the papilla and dental determinant.

Conclusions

We have constructed a model mechanism of the epithelial cell layer behaviour in the developing alligator jaw that predicts the formation of the dental determinant in the anterior of the jaw. The placode forms as a result of the assumptions made about the age structure of the epithelial cell layer, and the age dependency of CAM production. The asymmetrical spatial positioning of the placode is a result of jaw growth and the asymmetrical age structure of the cells.

The principal result of this paper is that the initiation of the dental determinant may be a result of jaw growth and the mechanical forces between the epithelial cells only if a certain restriction is met. This is that CAM levels must rise quickly in the neighbourhood of the dental determinant immediately prior to the development of the placode; a gradual increase in CAM levels over portions of the jaw anterior would be inconsistent with this model.

This restriction is not intuitively obvious from an analysis of the model on a fixed domain—it underlines the importance of domain growth as a morphogenetic variable. Very little previous work on pattern formation has included a study of the effects of domain growth on pattern development in reaction–diffusion systems. Notable exceptions are Lacalli (1981), Harrison *et al.* (1981), Harrison & Kolář (1988), and Arcuri & Murray (1986). As mentioned above, more recently some work has been done on a chemotaxis system with domain growth in which different pattern-forming scenarios (compared with a fixed domain) arise.

FUTURE WORK

This paper is a detailed discussion only of those aspects of the model that are relevant to the initiation of the dental determinant. Although much work remains to be done in the modelling of the specific tissue interaction processes, the formation of the papilla underlying the placode, and the development of the subsequent teeth, we give here a brief outline of how the model will be extended to deal with these processes to give an idea of how the model fits into a larger framework that explores the dependency of tooth initiation on jaw growth.

(i) The most important assumption is that the increased epithelial cell density in the region of the placode acts as a switch, inducing cell condensation in the mesenchyme. The exact mechanism of this induction is not known, but may be

mediated (among other things) by Hox-8 and Hox 7·1. We make the simple assumption that the raised epithelial cell density stimulates the production of a chemical (substance X) in the mesenchyme that induces cell condensation by a chemotactic process.

(ii) Substance X is assumed to stimulate the production of CAM in the epithelium, reinforcing the placode formation, and giving the mesenchyme odontogenic potential.

(iii) As the jaw grows, CAM production will be high everywhere, and thus tooth initiation will depend on the development of instabilities in the model equations. In turn these instabilities will develop only when the distance between two teeth is large enough, leading to a growth-dependent tooth initiation mechanism.

Thus, the full model will include a set of mechanochemical and diffusion equations for the mesenchyme as well as the ones described here for the epithelium. Solution of the model equations will have to be on a growing domain of increasing complexity. As models necessarily become more biologically realistic, their complexity clearly increases. Tissue interaction models for other skin organ primordia that have been proposed and studied (Nagorcka *et al.*, 1987; Cruywagen & Murray, 1992; Murray, 1992) make this clear.

We thank Dr Daniel Bentil for his help with some of the numerical work. A. Atri was supported by the Committee on Research of the Academic Senate of the University of California, Los Angeles. J. Sneyd and J. D. Murray were supported by NSF grant DMS-9106848. M. A. Lewis was supported in part by the National Sciences and Engineering Research Council of Canada. W. L. Seward was supported in part by the Natural Sciences and Engineering Research Council of Canada and the Information Technology Research Centre of Ontario.

APPENDIX

Here we develop some mathematical aspects of the model that are not essential for an understanding of the model results and predictions.

Our ultimate goal is to develop a model for the dental epithelium that produces a local increase in cell density (a "bump") at a point towards the front of the jaw. This bump may then be interpreted as the placode of the dental determinant. We start by showing how the model on a fixed domain can produce a spontaneous local increase in cell density in the *middle* of the domain, that is, a symmetrical bump. We then discuss how the model may be extended to a growing domain in such a way that the bump spontaneously appears in a region towards the front of the jaw.

Model Equations for a Fixed Domain

As described in the main text, the model equations for a fixed domain are

$$\frac{\partial n}{\partial t} = -\frac{\partial}{\partial x}\left(n\frac{\partial u}{\partial t}\right) \tag{A.1}$$

$$\frac{\partial}{\partial x}\left[\mu\frac{\partial^2 u}{\partial x\partial t}+E\frac{\partial u}{\partial x}+\frac{n}{1+\lambda n^2}\tau(c)\right]=\sigma un \tag{A.2}$$

$$\frac{\partial c}{\partial t}=\alpha\frac{\partial^2 c}{\partial x^2}-kc+F(u_x), \tag{A.3}$$

where n is the epithelial cell density, u is the displacement of epithelial cells from the resting state, c is the concentration of the cellular adhesion molecule, μ and E are, respectively, the viscosity and Young's modulus of the epithelial cell layer, and λ, σ, α and κ are constants. Equations (A.1) and (A.2) are the standard equations of motion for a visco-elastic fluid and are discussed in detail elsewhere (Murray, 1989; Murray *et al.*, 1983). Equation (A.3) is a reaction–diffusion equation for the concentration of the CAM and is coupled to the other two equations by the strain-dependent production term, $F(u_x)$. The qualitative shapes of $F(u_x)$ and $\tau(c)$ are given in Figs 2 and 3 in the main text: the functional forms used in the model are

$$\tau(c)=\tau_0-\tau_1 c_0+\tau_1 C$$

$$F(u_x)=\begin{cases}2F_0, & u_x\le -F_0/F_1\\ F_0-F_1u_x, & -F_0/F_1<u_x<F_0/F_1\\ 0, & F_0/F_1\le u_x\end{cases}$$

with constants, τ_0, τ_1, F_0 and F_1, and where $c_0=F_0/k$.

A homogeneous steady state of the model is given by $n=n_0$, $u=0$ and $c=F_0/k$ for some constant n_0. This corresponds to an unstressed state. Note that n_0 is not determined uniquely by the system of equations. Rather, the actual value for n_0 obtained for any given physical system is dependent on the physical properties of that system; we can thus consider n_0 as fixing the unperturbed state of the system under consideration.

Non-dimensional model

For computational and analytical work it is useful to non-dimensionalize the system of equations. Let L be some reference length (which in this case is related to the length of the jaw) and set $u^*=u/L$, $x^*=x/L$, $n^*=n/n_0$, $t^*=tE/\mu$, $\lambda^*=\lambda n_0^2$, $\tau_0^*=\tau_0 n_0/E$, $\tau_1^*=\tau_1 n_0 F_0/(kE)$, $\sigma^*=\sigma n_0 L^2/E$, $c^*=ck/F_0$, $\gamma_c=E/(k\mu)$, $\alpha^*=\alpha/(kL^2)$, $\kappa=F_1/F_0$. Substituting these into (A.1–A.3) and dropping the asterisks for algebraic simplicity gives

$$n_t+(nu_t)_x=0 \tag{A.4}$$

$$u_{xxt}+u_{xx}+\left[\frac{n\tau(c)}{1+\lambda n^2}\right]_x=\sigma un \tag{A.5}$$

$$\gamma_c c_t=\alpha c_{xx}-c+F(u_x) \tag{A.6}$$

where

$$F(u_x)=\begin{cases}2, & u_x\le -1/\kappa\\ 1-\kappa u_x, & -1/\kappa<u_x<1/\kappa\\ 0, & 1/\kappa\le u_x\end{cases}$$

and

$$\tau(c) = \tau_0 - \tau_1 + \tau_1 c.$$

Partial derivatives are denoted by subscripts.

Linear stability analysis

We determine the linear stability of the homogeneous steady state by looking for solutions of the form $\exp(\xi t + ilx)$ and solving for the eigenvalue, ξ, as a function of the wavenumber, l, such that non-trivial solutions exist. (For more details of this procedure see Murray, 1989.) Those values of l for which $\xi > 0$, give unstable wave modes, while those values of l for which $\xi < 0$, give stable wave modes. Standard linear analysis shows that, for any given wavenumber, ξ is given by the roots of

$$A(l)\xi^2 + B(l)\xi + C(l) = 0 \tag{A.7}$$

where

$$A(l) = \gamma_c l^2$$

$$B(l) = \alpha l^4 + \left[1 + \gamma_c - \frac{\gamma_c \tau_0 (\lambda - 1)^2}{1 + \lambda^2}\right] l^2 + \gamma_c \sigma$$

and

$$C(l) = \left[1 - \frac{\tau_0(\lambda - 1)^2}{1 + \lambda^2}\right] \alpha l^4 + \left[1 + \alpha\sigma - \frac{\tau_0((\lambda - 1)^2 + \kappa\tau_1)}{1 + \lambda^2}\right] l^2 + \sigma.$$

Determining the linear stability of any mode thus reduces the problem to finding the roots of the above quadratic, the dispersion relation.

Development of a symmetrical aggregation

Consider the model on a fixed dimensionless length of 1, corresponding to a dimensional length of L. If we choose the parameters such that the wavenumber $l = 2\pi$ is unstable, while all other wavenumbers $l = n\pi$, $n \neq 2$, are stable, then the linear instability generates the spatial pattern shown in Fig. 3 in the text. The dimensionless parameters used are $\tau_0 = 0{\cdot}7$, $\tau_1 = 0{\cdot}1$, $\lambda = 0{\cdot}1$, $\gamma_c = 0{\cdot}1$, $\kappa = 15{\cdot}0$, $\alpha = 0{\cdot}01$ and $\sigma = 6{\cdot}13$. A graph of the dispersion relation for these parameters is given in Fig. A1. The parameter values were found using the logical parameter search method developed by Bentil & Murray (1991).

Initial and boundary conditions

As initial conditions we assume that the epithelial cell densities and CAM concentrations exhibit small amplitude variations about their steady-state values. We also assume that the cells are initially unstressed, that is, that $u = 0$.

At the boundaries of the domain we assume no-flux conditions for n and c, that is, we assume that neither the epithelial cells nor the CAM are able to move out of the

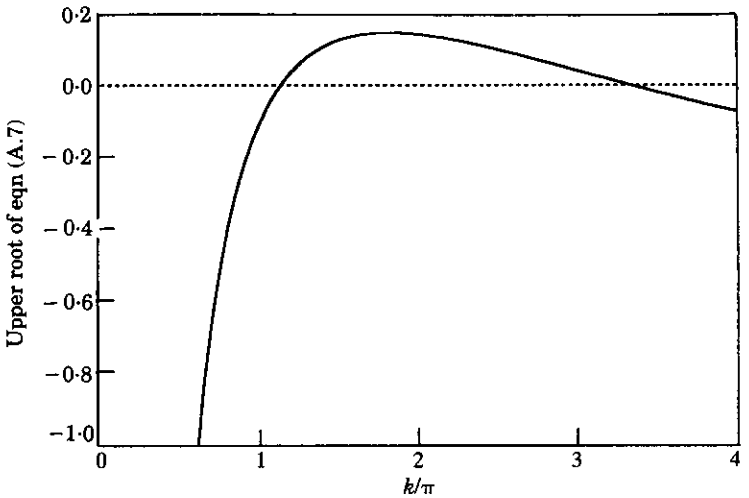

FIG. A1. Dispersion relation for the model with the parameters given in the Appendix. This curve is the greater root of (A.7), ξ_+ say, as a function of l/π. Note how $\xi_+(2) > 0$, i.e. the mode corresponding to $\cos(2\pi x)$ is unstable, resulting in the stable spatial pattern shown in Fig. 3.

domain. We assume further that u is fixed at zero at the boundaries that is, that the boundaries are unstressed.

Numerical methods

All of our computations were performed using the SPRINT package of Fortran subroutines (Berzins & Furzeland, 1985, 1986) and checked with the routine D03PGF from the NAG library. The SPRINT routines use a lumped infinite element method to discretize the model equations in space and are often more robust for non-linear problems than the centred finite differences used in D03PGF. In either case, it is necessary to add the equation $u_t = w$ to the previous set (A.4–A.6) to write the system in a standard form. Equation (A.5) becomes

$$w_{xx} + u_{xx} + \left[\frac{n\tau(c)}{1+\lambda n^2}\right]_x = \sigma u n,$$

and no longer includes a derivative with respect to time. Consequently, when the modified equations are discretized in space, a system of differential-algebraic equations results. Although differential-algebraic equations can be difficult to solve numerically this particular system is relatively uncomplicated and both SPRINT and the NAG library include integration routines that can solve it. The computations were performed in double precision on a DecStation 3100.

THE MODEL ON A GROWING DOMAIN

We now include the effects of jaw growth on the pattern formation process. By solving the equations on a growing domain we aim to demonstrate how the model

can result in an asymmetrical bump, one that appears skewed towards the front of the jaw, in a position analogous to the position of the dental determinant.

One relatively simple way to perform the computations on a growing domain is to let L, the characteristic length, be a function of time. Since the only dimensionless parameter groupings that depend on L are α and σ, this is equivalent to making α and σ functions of time. Fortunately, this does not change the linear stability analysis. A simple calculation shows that the dispersion relation remains invariant under the transformation

$$\alpha \to \alpha/\tilde{L}^2$$

$$\sigma \to \tilde{L}^2\sigma$$

$$l \to \frac{n\pi}{1/\tilde{L}} = n\pi\tilde{L}.$$

Thus, if we divide α by $\tilde{L}^2$, multiply σ by $\tilde{L}^2$, and solve the equations on the domain $[0, 1]$ as before, the same linear instability obtains in any interval of length $1/\tilde{L}$. This corresponds to solving the equations (with their original values for α and σ) on $[0, \tilde{L}]$, with the same linear instability holding in any interval of length 1. Note that the dimensionless interval $[0, \tilde{L}]$ corresponds to the dimensional length $[0, L\tilde{L}]$.

Stepwise solution of the model

We do not explicitly make σ and α functions of time. Instead we assume that the mechanical and chemical processes of the model act on a much smaller time scale than jaw growth. Thus, we solve the model equations by the following stepwise process:

(i) starting on the smallest domain size, $L = 1$, allow the model to reach a steady state, holding α and σ fixed;
(ii) step time forward by a relatively large increment, by increasing the domain size (i.e. scaling α and σ appropriately);
(iii) allow the model to reach a new steady state, holding α and σ fixed at their new values. For initial conditions, use the steady state from the previous step;
(iv) keep on increasing domain length in this way, until the desired length is reached.

Initial and boundary conditions

The initial conditions for the smallest domain length, $L = 1$, were random perturbations of n, u, and c about their mean values. As explained above, subsequent domains had as their initial conditions the steady-state solutions of the domains immediately preceding them.

The boundary conditions for all domain sizes were the same as those used for the model equations on a fixed domain, with the exception of the boundary condition for the CAM which was held fixed at zero at the rear of the jaw. This was intended to model phenomenologically the relative absence of CAMs at the rear of the jaw.

REFERENCES

ARCURI, P. & MURRAY, J. D. (1986). Pattern sensitivity to boundary and initial conditions in reaction-diffusion models. *J. math. Biol.* **24,** 141–165.

BELINTSEV, B. N., BELOUSSOV, L. V. & ZARAISKY, A. G. (1987). Model of pattern formation in epithelial morphogenesis. *J. theor. Biol.* **129,** 369–394.

BENTIL, D. E. & MURRAY, J. D. (1991). Pattern selection in biological pattern formation mechanisms. *Appl. Math. Lett.* **4,** 1–5.

BERZINS, M. & FURZELAND, R. M. (1985). *A users manual for SPRINT—a versatile software package for solving systems of algebraic, ordinary and partial differential equations: Part 1 Algebraic and ordinary differential equations.* Thornton: Thornton Research Centre, Shell Research Ltd.

BERZINS, M. & FURZELAND, R. M. (1986). *A users manual for SPRINT—a versatile software package for solving systems of algebraic, ordinary and partial differential equations: Part 2 Partial differential equations.* Thornton: Thornton Research Centre, Shell Research Ltd.

CHUONG, C.-M. & EDELMAN, G. M. (1985). Expression of cell-adhesion molecules in embryonic induction. I. Morphogenesis of nestling feathers. *J. Cell Biol.* **101,** 1009–1026.

CRUYWAGEN, G. & MURRAY, J. D. (1992). On a tissue interaction model of biological pattern formation. *J. Nonlin. Sci.* **2,** 217–240.

DHOUAILLY, D. (1975). Formation of cutaneous appendages in dermoepidermal recombination between reptiles, birds and mammals. *Wilh. Roux Arch. Entw. Mech. Org.* **177,** 323–340.

EDMUND, A. G. (1960). Tooth replacement phenomena in the lower vertebrates. *Contrib. Life Sci. Div. Roy. Ont. Mus.* **52,** 1–90.

EDMUND, A. G. (1962). Sequence and rate of tooth replacement in the Crocodilia. *Contrib. Life Sci. Div. Roy. Ont. Mus.* **56,** 1–42.

FOLKMAN, J. & MOSCONA, A. (1978). Role of cell shape in growth control. *Nature, Lond.* **273,** 345–349.

HARRIS, A. K. (1982). Traction and its relation to contraction in tissue cell locomotion. In: *Cell Behaviour* (Bellairs, R., Curtis, A. & Dunn, G., eds) pp. 109–134. Cambridge: Cambridge University Press.

HARRIS, A. K., STOPAK, D. & WILD, P. (1981). Fibroblast traction as a mechanism for collagen morphogenesis. *Nature, Lond.* **290,** 249–251.

HARRIS, A. K., WILD, P. & STOPAK, D. (1980). Silicon rubber substrata: a new wrinkle in the study of cell locomotion. *Science* **208,** 177–179.

HARRISON, L. G. & KOLÁŘ, M. (1988). Coupling between reaction-diffusion prepattern and expressed morphogenesis, applied to Desmids and Dasyclads. *J. theor. Biol.* **130,** 493–515.

HARRISON, L. G., SNELL, J., VERDI, R., VOGT, D. E., ZEISS, G. D. & GREEN, B. R. (1981). Hair morphogenesis in *Acetabularia mediterranea*: temperature-dependent spacing and models of morphogen waves. *Protoplasma* **106,** 211–221.

KOLLAR, E. J. (1981). Tooth development and dental patterning. In: *Morphogenesis and Pattern Formation* (Connelly, T. G., *et al.*, eds). New York: Raven Press.

KOLLAR, E. J. & BAIRD, G. R. (1969). The influence of the dental papilla on the development of tooth shape in embryonic mouse tooth germs. *Embryol. exp. Morphol.* **21,** 131–148.

KOLLAR, E. J. & BAIRD, G. R. (1970*a*). Tissue interactions in embryonic mouse germs. I. Reorganization of the dental epithelium during tooth-germ reconstruction. *Embryol. exp. Morphol.* **24,** 159–171.

KOLLAR, E. J. & BAIRD, G. R. (1970*b*). Tissue interactions in embryonic mouse germs. II. The inductive role of the dental papilla. *Embryol. exp. Morphol.* **24,** 173–186.

KOLLAR, E. J. & LUMSDEN, A. G. S. (1979). Tooth morphogenesis: the role of the innervation during induction and pattern formation. *J. Biol. Buccale* **7,** 49–60.

KRONMILLAR, J. E., UPHOLT, W. B. & KOLLAR, E. J. (1991). EGF Antisense oligodeoxynucleotides block murine odontogenesis *in vitro*. *Dev. Biol.* **147,** 485–488.

LACALLI, T. C. (1981). Dissipative structures and morphogenetic pattern in unicellular algae. *Phil. Trans. R. Soc. Lond. B* **294,** 547–588.

LUMSDEN, A. G. S. (1979). Pattern formation in the molar dentition of the mouse. *J. Biol. Buccale* **7,** 77–103.

LUMSDEN, A. G. S. (1988). Spatial organization of the epithelium and the role of neural crest cells in the initiation of the mammalian tooth germ. *Development* (Supplement) **103,** 155–169.

MACKENZIE, A., FERGUSON, M. J. W. & SHARPE, P. T. (1991*a*). Hox-7 expression during murine craniofacial development. *Development* **113,** 601–611.

MACKENZIE, A., FERGUSON, M. J. W. & SHARPE, P. T. (1992). Expression patterns of the homeobox gene, Hox-8, in the mouse embryo suggest a role in specifying tooth initiation and shape. *Development* **115,** 403–420.

MACKENZIE, A., LEEMING, G. L., JOWETT, A. K., FERGUSON, M. J. W. & SHARPE, P. T. (1991*b*). The homeobox gene Hox 7·1 has specific regional and temporal expression patterns during early murine

craniofacial embryogenesis, especially tooth development *in vitro* and *in vitro. Development* **111,** 269–285.

MAINI, P. K., MYERSCOUGH, M. R., WINTERS, K. H. & MURRAY, J. D. (1991). Bifurcating spatially heterogeneous solutions in a chemotaxis model for biological pattern generation. *Bull. math. Biol.* **53,** 701–719.

MINA, M. & KOLLAR, E. J. (1987). The induction of odontogenesis in non-dental mesenchyme combined with early murine mandibular arch epithelium. *Archs. oral Biol.* **32,** 123–127.

MURRAY, J. D. (1989). *Mathematical Biology.* London: Springer-Verlag.

MURRAY, J. D. (1993). Complex pattern formation and tissue interaction. In: *Proc. Ist European Conference on the Applic. Math. to Medic. & Biol.* (Demongeot, J. & Capasso, V., eds). Heidelberg: Springer-Verlag, in press.

MURRAY, J. D., OSTER, G. F. & HARRIS, A. K. (1983). A mechanical model for mesenchymal morphogenesis. *J. math. Biol.* **17,** 125–129.

MURRAY, J. D. & OSTER, G. F. (1984*a*). Generation of biological pattern and form. *IMA J. Math. Appl. Medic. Biol.* **1,** 51–75.

MURRAY, J. D. & OSTER, G. F. (1984*b*). Cell traction models for generating pattern and form in morphogenesis. *J. math. Biol.* **19,** 265–279.

MURRAY, J. D., MAINI, P. K. & TRANQUILLO, R. T. (1988). Mechanical models for generating biological pattern and form in development. *Phys. Reports* **171,** 60–84.

NAGORCKA, B. N., MANORANJAN, V. S. & MURRAY, J. D. (1987). Complex spatial patterns from tissue interactions—an illustrative model. *J. theor. Biol.* **128,** 359–374.

OBRINK, B. (1986). Epithelial cell adhesion molecules. *Exp. Cell Res.* **163,** 1–21.

ODELL, G., OSTER, G. F., BURNSIDE, B. & ALBERCH, P. (1981). The mechanical basis for morphogenesis. *Devel. Biol.* **85,** 446–462.

OSBORN, J. W. (1970). New approach to Zahnreihen. *Nature, Lond.* **225,** 343–346.

OSBORN, J. W. (1971). The ontogeny of tooth succession in *Lacerta vivipara* Jacquin (1787). *Proc. R. Soc. Lond. B* **179,** 261–289.

OSBORN, J. W. (1978). Morphogenetic gradients: fields versus clones. In: *Development, Function and Evolution of Teeth* (Butler, D. M. & Joysey, K. A., eds). London: Academic Press.

OSBORN, J. W. (1979). A cladistic interpretation of morphogenesis. *J. Biol. Bucc.* **6,** 327–337.

OSBORN, J. W. (1984). From reptile to mammal: evolutionary considerations of the dentition with emphasis on tooth attachment, *Symp. zool. Soc. Lond.* **52,** 549–574.

OSTER, G. F., MURRAY, J. D. & HARRIS, A. K. (1983). Mechanical aspects of mesenchymal morphogenesis. *J. Embryol. exp. Morphol.* **78,** 83–125.

OSTER, G. F., MURRAY, J. D. & MAINI, P. K. (1985). A model for chrondrogenic condensations in the developing limb: the role of extracellular matrix and cell tractions. *J. Embryol. exp. Morphol.* **89,** 93–112.

PARTANEN, A.-M. & THESLEFF, I. (1989). Growth factors and tooth development. *Int. J. Dev. Biol.* **33,** 165–172.

RÖSE, C. (1894). Ueber die Zahnentwicklung der Crocodile. *Morph. Arbeit.* **3,** 195–228.

TAKEICHI, M. (1988). The cadherins: cell-cell adhesion molecules controlling animal morphogenesis. *Development* **102,** 639–655.

THESLEFF, I. & HURMERINTA, K. (1981). Tissue interactions in tooth development. *Differentiation* **18,** 75–88.

THESLEFF, I., JALKANEN, M., VAINIO, S. & BERNFIELD, M. (1988). Cell surface proteoglycan expression correlates with epithelial-mesenchymal interaction during tooth morphogenesis. *Dev. Biol.* **129,** 565–572.

THESLEFF, I., VAINIO, S. & JALKANEN, M. (1989). Cell-matrix interactions in tooth development. *Int. J. Dev. Biol.* **33,** 91–97.

TURING, A. M. (1952). The chemical basis of morphogenesis. *Phil. Trans. R. Soc. Lond. B* **237,** 37–72.

WESTERGAARD, B. & FERGUSON, M. W. J. (1986). Development of the dentition in *Alligator mississippiensis.* Early embryonic development in the lower jaw. *J. Zool. Lond.* **210,** 575–597.

WESTERGAARD, B. & FERGUSON, M. W. J. (1987). Development of the dentition in *Alligator mississippiensis.* Later development in the lower jaws of embryos, hatchlings and young juveniles. *J. Zool. Lond.* **212,** 191–222.

WESTERGAARD, B. & FERGUSON, M. W. J. (1990). Development of the dentition in *Alligator mississippiensis.* Upper jaw dental and craniofacial development in embryos, hatchlings and young juveniles. *Am. J. Anatomy* **187,** 393–421.

WOERDEMAN, M. W. (1919). Beiträge zur Entwicklungsgeschichte von Zähnen und Gebiss der Reptilien. Beitrag I. Die Anlage und Entwichlung des embryonalen Gebisses als Ganzes und seine Beziehung zur Zahnleiste. *Arch. Mikrosk. Anat.* **92,** 104–192.

WOLPERT, L. (1969). Positional information and the spatial pattern of cellular differentiation. *J. theor. Biol.* **25**, 1–47.
WOLPERT, L. (1971). Positional information and pattern formation. *Curr. Top. Dev. Biol.* **6**, 183–224.
WOLPERT, L. (1981). Positional information and pattern formation. *Phil. Trans. R. Soc. Lond.* **B295**, 441–450.